

Athermalization Design of Dynamic Star Simulator Optical System

Fukang Xue*, Junfa Duan, Gaolin Qin, Wei Wei

*School of Mechanical Engineering, North China University of Water Resources and Electric Power,
Zhengzhou, 450003, China*

**corresponding author*

Keywords: Dynamic star simulator; Passive thermalization elimination; Athermalization; Imaging quality

Abstract: According to the working requirements of the dynamic star simulator, the optical passive thermalization elimination method is used to achieve the purpose of athermalization. Using CODE V optical software designed a set of refraction primary imaging optical system composed of different thermal characteristics materials and corrected axial aberration and other aberrations. The software used to analyze the imaging quality of the optical system at $-40^{\circ}\text{C} \sim 60^{\circ}\text{C}$, the results show that the optical system in the full temperature range of the diffuse diameter of $20.5\mu\text{m}$, better than the Airy disk diameter and pixel size ; The full field modulation transfer function is higher than the diffraction limit at a spatial frequency of 20lp/mm, and the imaging quality is excellent; the energy distribution is over 65%; The defocusing amount at each temperature is all less than the depth of focus, which satisfies the requirements of the star simulator.

1 Introduction

In recent years, the aerospace industry has developed rapidly, and the use of space vehicles has become more and more widespread. With the development of space technology and the improvement of aircraft attitude positioning requirements, star sensors, as high-precision space attitude measurement equipment for capturing and measuring their flight attitude information in space vehicles [1-2], have increasingly higher technical requirements. The star simulator, as a device for accurately simulating the position of stars in the sky on the ground of a star sensor, has also received more and more attention [3].

In order to adapt to the extreme environment and further ensure the test performance of the star simulator, it is necessary for the star simulator to meet the requirements of use in an environment of $-40^{\circ}\text{C} \sim 60^{\circ}\text{C}$. When entering the environment of $-40^{\circ}\text{C} \sim 60^{\circ}\text{C}$, due to temperature changes, the refractive index and structural parameters of the optical system will change [4], which will cause the focal length of the system to change, and the image surface will shift, resulting in degradation of

system performance and image quality. Therefore, it is quite necessary to conduct athermal design in the design process of dynamic star simulator [5].

2 Optical System Design

2.1 Design Principle

There are currently three types of athermalization technologies: mechanical passive, electromechanical active and optical passive. By comparing the advantages and disadvantages of the three methods, optical passive defocusing can not only ensure the use of appropriate material combination to compensate thermal defocusing, but also has the advantages of small size, relatively simple structure, light weight and high system reliability, so it has been widely used in the design of thermal defocusing [6].

The principle of optical passive athermalization technology is that when the temperature changes, the amount of defocus produced by the optical element and the amount of change produced by the mechanical structure compensate each other, so as to ensure the stability of the image plane. In addition to satisfying the principle of reasonable distribution of optical focus and achromatic requirements, the optical system should also have the ability of thermal desorption. Three equations of thermal desorption design can be established, namely, the distribution relation of optical focus, the achromatic condition and the thermal desorption condition for compensating image plane defocusing.

The optical system should satisfy the following equation [7]:

$$\phi = \frac{1}{h_1} \sum_{i=1}^n h_i \phi_i \quad (1)$$

$$\Delta f_b^T = \left(\frac{1}{h_1 \phi} \right)^2 \sum_{i=1}^n (h_i^2 \omega_i \phi_i) = 0 \quad (2)$$

$$df_b^T / dt = \left(\frac{1}{h_1 \phi} \right)^2 \sum_{i=1}^n (h_i^2 \chi_i \phi_i) = \alpha_h L \quad (3)$$

Where, ϕ_i is the optical focus of each lens group; ϕ for the total light focus of the system; h_1 is the height of the first paraxial ray at each lens group; ω_i is the dispersion factor of each lens group, that is, the relative change of optical focus caused by dispersion; χ_i is the photothermal expansion coefficient, that is, the change rate of focal length caused by temperature; α_h is the thermal expansion coefficient of the mechanical structure. L is the length of the mechanical structure.

The coefficient of the combined refractive lens is [8]:

$$x_{f,r} = \alpha - \frac{1}{n-n_0} \left(\frac{dn}{dT} - n \frac{dn_0}{dT} \right) \quad (4)$$

Where, α is the thermal expansion coefficient of the optical material; n is the refractive index of the optical element; dn/dT is the temperature refractive index coefficient of the material; dn_0/dT is the temperature refractive index coefficient of the medium.

From equation (4), it can be seen that the thermal expansion coefficient and refractive index temperature coefficient of the material are the determining factors of the temperature characteristics of the refraction element. At the same time, it can be concluded that the thermal difference coefficient of the refraction element is negative or positive. Therefore, through reasonable design,

different positive and negative refraction elements can be combined to compensate each other so as to satisfy the equations (1), (2) and (3) to achieve the purpose of athermalization.

2.1.1 Design Requirements

According to the index requirements, a display device with a resolution of 1080×1200 and a pixel size of $23.2 \mu\text{m} \times 46.4 \mu\text{m}$ is selected. The relevant design parameters are shown in Table 1.

Table 1: Optical system indicators.

Parameter	Index
wavelength	$0.6\mu\text{m} \sim 0.8\mu\text{m}$
focal length	68.8mm
Field of view	$\geq 40^\circ$
Exit pupil distance	$\geq 40\text{mm}$
MTF	$\geq 0.8 @ 20\text{lp/mm} \& 40^\circ \text{FOV}$
Airy disk diameter	$39.2\mu\text{m}$

2.1.2 Design result

According to the index requirements, use CODE V to design an optical system that meets the index. The structure of the system is shown in Figure 1.

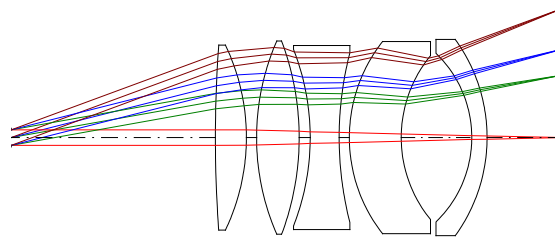


Figure 1: 2D layout of the optic system.

The optical system was further optimized on the basis of reference patent. The refraction imaging mode was adopted. The lens material was HK51 and HZF4A, and the thermal difference coefficients were $1.4 \times 10^{-6}/^\circ\text{C}$ and $-1.5 \times 10^{-6}/^\circ\text{C}$, respectively. The lens barrel material is aluminum alloy. CODE V software was used to analyze and evaluate the performance and imaging quality of the system at -40°C , 20°C , and 60°C .

3 System Image Quality Evaluation

3.1 System Image Quality at 20°C

Figure 2 shows the dot plot of the optical system at 20°C , representing the size of the dispersion speckle focused on the imaging surface after the parallel beam passes through the optical system. The imaging quality can be seen by observing the density and size of the dispersion speckle in the dot plot, which usually requires small dry Airy speckle. It can be seen from the figure that the

optimized edge field of view (20°) has a little color difference, but the RMS value of the dispersion spot is 9.655 μm , and the diameter of the dispersion spot is 17.9 μm , which is better than Airy spot diameter and the pixel size of the display.

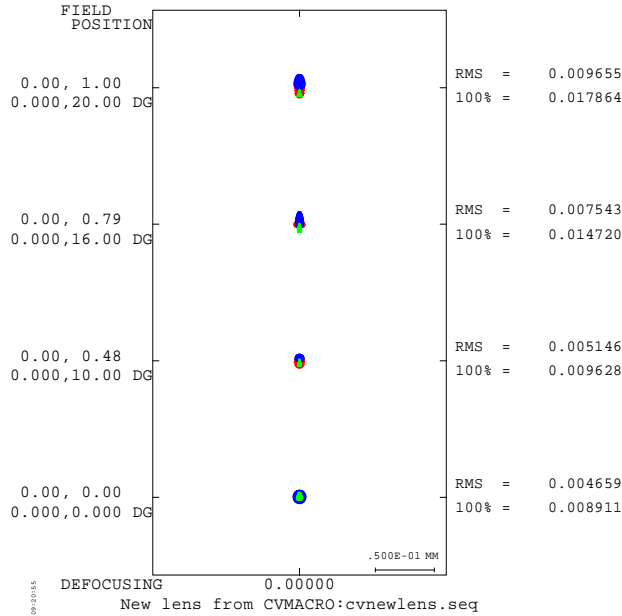


Figure 2: Spot diagram.

Figure. 3 is a graph of the modulation transfer function of the optical system. When the full field of view MTF curve of the system is 20lp/mm at the Nyquist frequency, the MTF value of the full field of view is better than the diffraction limit value, reaching above 0.84.

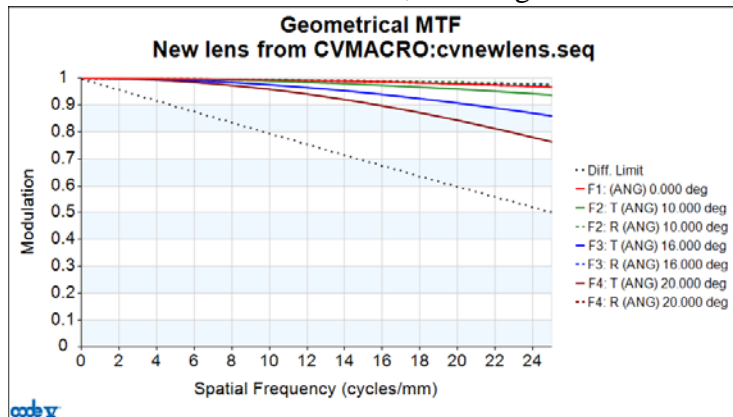


Figure 3: MTF curves of the system.

Fig. 4 is a graph of the enveloping energy of the optical system. It can be seen from the figure that more than 65% of the energy in the full field of view is concentrated in the smallest pixel 23.2 μm of the display device. Since the entrance pupil diameter is 3mm, there is diffraction phenomenon, but the energy transmittance still meets the requirements of use.

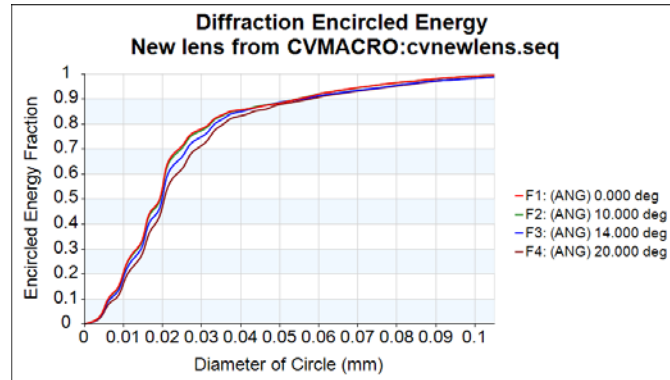


Figure 4: Encircled Energy Fraction.

From the above analysis, it can be seen that the optical system has good performance at 20°C, the overall geometric aberration and chromatic aberration are well corrected, and various indicators such as the MTF curve and the energy distribution rate meet the requirements of use.

3.2 Imaging Quality of the System as Temperature Changes

According to the operating temperature requirements of the star simulator, when the system is at -40°C~60°C, in order to avoid the influence of temperature changes on the imaging quality of the system and to further ensure the performance of the system, it is necessary to conduct thermal analysis on the optical system.

Taking extreme temperatures of -40°C and 60°C as analysis nodes, if the system meets the index requirements at -40°C and 60°C, it will meet the requirements for use at the entire operating temperature. The design results are simulated and analyzed using CODE V software.

It can be seen from Figures 5~8 that the maximum diameter of the diffuse spot is 21.2μm, and the maximum RMS value is 11.6μm, which are both smaller than the Airy disk diameter and the minimum size of the display pixel. At the same time, the modulation transfer function in the full field of view is better than the diffraction limit value at the spatial frequency of 20lp/mm, reaching above 0.76. By comparing the image quality of -40°C, 20°C and 60°C, it can be seen that the performance of the system meets the requirements of use at the entire operating temperature.

Figure 5 and Figure 6 show the system point diagram and MTF diagram at -40°C.

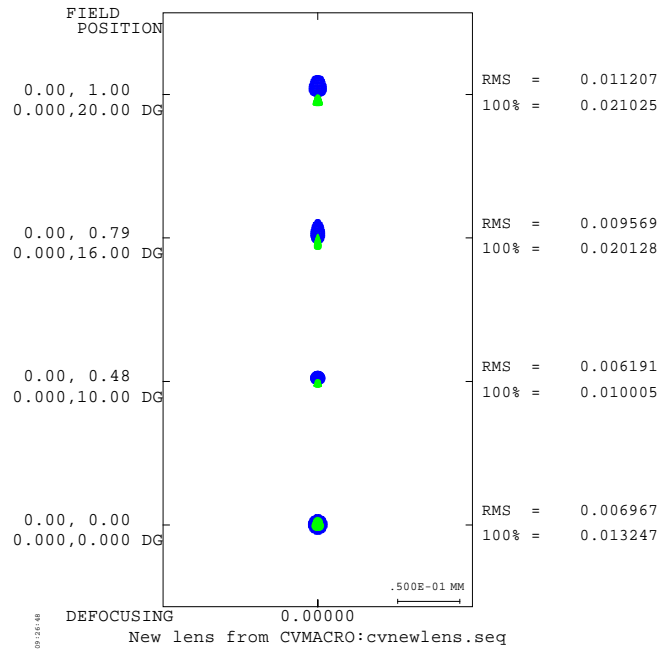


Figure 5: Spot diagram of -40°C.

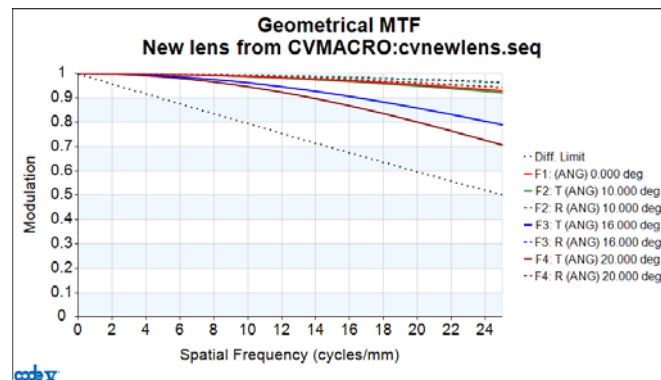


Figure 6: MTF curves of the system -40°C.

Figure 7 and Figure 8 show the system point diagram and MTF diagram at 60°C.

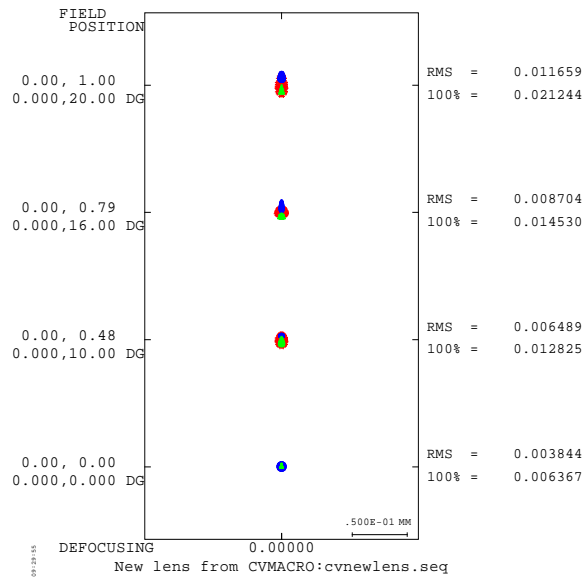


Figure 7: Spot diagram of 60°C.

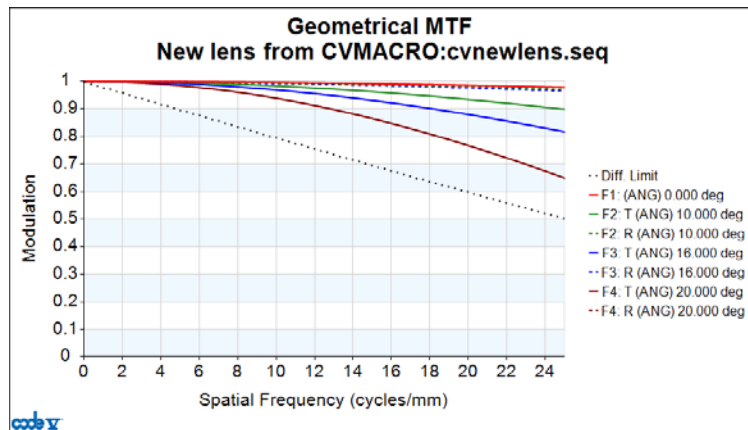


Figure 8: MTF curves of the system 60°C.

Through the above simulation analysis, it can be concluded that the imaging quality of the optical system is still good in the range of working temperature $-40^{\circ}\text{C}\sim 60^{\circ}\text{C}$, and the maximum defocus is less than the focal depth of $55\mu\text{m}$ through the combination of different positive and negative lenses, so the purpose of passive thermal desorption is achieved. Table 2 shows the change value of the defocus of the system at different temperatures.

Table2 System defocusing at different temperatures.

Temperature / $^{\circ}\text{C}$	-40°C	-20°C	0°C	20°C	40°C	60°C
Defocus / μm	21.2	14.2	7.1	0	-7.1	-14.1

4. Summary

According to the working requirements of the star simulator, this paper uses CODE V to design the optical system, adopts the method of optical passive heat dissipation to achieve the purpose of

athermalization, and at the same time, through the combination of materials with different thermal characteristics, it is used to eliminate axial chromatic aberration and other aberrations. Use software to analyze the imaging quality of the optical system at $-40^{\circ}\text{C}\sim 60^{\circ}\text{C}$. The results show that in the whole temperature range, the maximum dispersion spot diameter is $20.5\mu\text{m}$, the maximum RMS value is $11.1\mu\text{m}$, which are better than Airy spot diameter and the pixel size of the display. The image quality of MTF curve is higher than the diffraction limit at the space frequency of 20lp/mm , and the energy distribution reaches more than 65%. The optical system has simple structure and high reliability, and meets the requirements of the use of a star simulator.

Reference

- [1] Li Xuekui, Hao Zhihang, Li Jie, et al. (2004) *The research on the method of the star's position determination of the star sensor*. *Chinese J Electron Devices*, 27(4): 571-574.
- [2] Li Jing, Yang Baoxi, Hu Zhonghua, et al. (2013) *Development and performance testing of optical system for star sensor*. *Acta Optica Sinica*, 33(5): 0522005.
- [3] Chen Qimeng, ZhangGuoyu, Wang, Zhe, Zhang, et al. (2014) *Optical System Design of High-Precision Static Star Simulator with Large Field of View*. *Laser & Optoelectronics Progress*, 51(5).
- [4] Zhang Faqiang, Fan Xiang, Kong Hui, et al. (2015) *Influence of temperature on infrared optical system and athermal design*. *Infrared and Laser Engineering*. 45(7): 854-860.
- [5] LIU Ruiqi, CHEN Xingming, ZHAO Jiacyi. (2009) *Design of a compact infrared optical system*. *Laser & Infrared*, 39(4):419-422.
- [6] BAI Yu, YANG Jianfeng, MA Xiaolong, et al. (2009) *An Athermal Design of Infrared Hybrid Diffractive/Refractive Optical System in $3.7\text{-}4.8\mu\text{m}$* . *Acta Photonica Sinica*, 38(9): 2261—2264.
- [7] SUN Qiang, LIU Hongbo, WANG Zhaoqi, et al. (2003) *An infrared diffractive / refractive optical system beyond normal temperature*. *Acta Photonica Sinica*, 32(4): 466—469.
- [8] H.P. Helzik, Helzik, Zhou Haixian. (2002) *Micro-optical components, systems and applications*. National Defense Industry Press.